SAE INTERNATIONAL

ARTICLE INFO
Article ID: 07-11-01-0007

doi:10.4271/07-11-01-0007

2-D CFAR Procedure of Multiple Target Detection for Automotive Radar

Sen Li, Tongji University
Xin Bi, *Tongji University*
Libo Huang, *Automotive Sensors Group*
Bin Tan, *Tongji University*

Abstract

In Advanced Driver Assistant System (ADAS), the automotive radar is used to detect targets or obstacles around the vehicle. The procedure of Constant False Alarm Rate (CFAR) plays an important role in adaptive targets detection in noise or clutter environment. But in practical applications, the noise or clutter power is absolutely unknown and varies over the change of range, time and angle. The well-known cell averaging (CA) CFAR detector has a good detection performance in homogeneous environment but suffers from masking effect in multi-target environment. The ordered statistic (OS) CFAR is more robust in multi-target environment but needs a high computation power. Therefore, in this paper, a new two-dimension CFAR procedure based on a combination of Generalized Order Statistic (GOS) and CA CFAR named GOS-CA CFAR is proposed. Besides, the Linear Frequency Modulation Continuous Wave (LFMCW) radar simulation system is built to produce a series of rapid chirp signals. Then the echo signals are converted into a two-dimensional Range-Doppler matrix (RDM), which contains information about the targets as well as background clutter and noise, through twice Fast Fourier Transform (FFT).The simulation experimental results show that compared to the two-dimensional OS-CA CFAR, the new 2-D GOS-CA CFAR can enhance the detection performance and robustness in the actual multi-target environment with lower computational complexity.

History

Received: 12 Jan 2018
Published: 23 Sep 2017
e-Available: 23 Sep 2017

Citation

Li, S., Bi, X., Huang, L., and Tan, B., "2-D CFAR Procedure of Multiple Target Detection for Automotive Radar," *SAE Int. J. Passeng. Cars – Electron. Electr. Syst.* 11(1):2018, doi:10.4271/07-11-01-0007.

ISSN: 1946-4614
e-ISSN: 1946-4622





Introduction

With the rapid development of vehicle electronic technology, the Advanced Driver Assistance System (ADAS) has attracted extensive attention. As a key sensor, automotive radar has already been used in many current passenger cars, trucks and buses. Available commercial products are equipped with safety and comfort functions like Autonomous Emergency Braking(AEB), Blind Spot Detection(BSD), and Adaptive Cruise Control(ACC), which are all realized with the help of compact radar sensors. Hence, using millimeter wave radar to detect front targets and obstacles is an important part of ADAS system for environmental perception around vehicles.

Target detection can usually be regarded as a two-element hypothesis test for judging whether there is a target in the observation. In radar systems, the CFAR procedure is widely used to detect targets. Method of CFAR detection is to determine whether the cell has a target by comparing the signal of detection cell and the CFAR threshold which can be obtained through the estimation of background noise and clutter power. In general, the average noise and clutter power cannot be obtained directly and therefore has to be estimated. To estimate the average noise power, a lot of CFAR algorithms and processes have been proposed to get adaptive, fast and robust detection performance.

The cell average (CA) algorithm [1] which is proposed firstly in 1968 belongs to the mean level (ML) CFAR algorithm. The common feature of ML-CFAR is the mean method used in the local estimation, which has a good detection performance and less CFAR loss in a single target and homogeneous background noise. In order to improve the detection performance in nonhomogeneous clutter background, some algorithms such as GO [2], SO [3], WCA [4,5] and some detectors [6] were proposed, which belong to ML CFAR. However, when the automotive radar detects multiple targets in front like vehicles or pedestrians, a plurality of targets with different power will appear in the reference window. In this case, the detection threshold will be raised, and the target with low power will be masked. Another representative CFAR detector is order statistics(OS) CFAR proposed by Rohling in1983[7]. The OS CFAR detector has better interference suppression capability than the ML CFAR detector in the multi-target environment, and is also acceptable in both the homogeneous clutter background and the clutter edge environment [8]. Besides, the Censored Mean Level Detector (CMLD) was proposed by Richard and Dillard in 1977 [9], which used threshold compensation techniques and could be considered as OS CFAR detector. But OS CFAR requires a lot of computation, especially when the number of reference window is large. Based on the advantages of one-dimensional CA and OS CFAR, a two-dimensional (2-D) OS-CA and FOS-CA CFAR was proposed by Rohling and Kronauge [10]. 2-D CFAR makes it more accurate to estimate the local background noise power by increasing the number of reference cells. So, in this paper, we focus on a two-dimensional fast Fourier transform (FFT)-based signal processing approach to establish Range-Doppler matrix (RDM) which can be easily realized using standard signal processing blocks already used in automotive radar systems. Then a new 2-D CFAR detector will be proposed.

The rest of this paper is organized as follows. Section 2 presents the basic CFAR processing. Section 3 presents the equation of waveform design and signal processing into Range-Doppler matrix(RDM). In section 4 the two-dimensional GOS-CA CFAR detector is proposed. In sections 5, performances of several detectors are compared.

CFAR Procedure

The conventional one-dimensional CFAR procedure is shown in figure 1.

It is assumed that all targets are fluctuating according to the Swerling I or II model, then Clutter is independent and identically distributed (IID) complex Gaussian Random processes. The signal samples are stored in a window divided into 2N, and in a Square-law detector each cell is composed of a signal sample, defined as:

$$y_n = |x_n|^2, n = 1,2\cdots \mathrm{N}. \qquad \text{Eq. (1)}$$

Where, $x_N = \{x_I, x_Q\}$ is the quadrature form of x_N.

The target detection procedure is described in following equation:

$$f(Y) = \begin{cases} H_1 & Y \geq T \\ H_0 & Y < T \end{cases} \qquad \text{Eq. (2)}$$

Where the hypothesis H_1 denotes that there is a target in the cell under test (signal plus noise and clutter) while hypothesis H_0 represents the noise and clutter alone which is denoted by Y_0.

In a square-law detector this random variable Y_0 is exponentially distributed with the following probability density function(pdf) and the average noise power is μ:

$$f(y) = \frac{1}{\mu}\exp\left(-\frac{y}{\mu}\right) \quad y \geq 0 \qquad \text{Eq. (3)}$$

FIGURE 1 Conventional adaptive Detection Scheme.

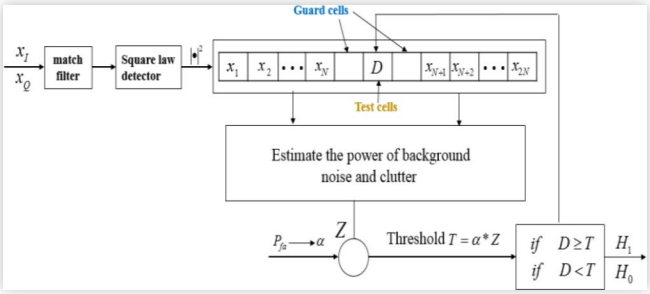

If there is a target in the test cell, the function can be described as follow, and s is Signal-to-Clutter Ratio (SCR) of target and clutter:

$$f(y)=\frac{1}{(1+s)\mu}\exp\left(\frac{-y}{(1+s)\mu}\right) \quad y\geq 0 \qquad \text{Eq. (4)}$$

Accordingly, the threshold T is always calculated as the product:

$$T=\alpha * Z \qquad \text{Eq. (5)}$$

Parameter α is the scaling factor used to control the false alarm probability P_{fa} and the parameter Z is the estimate for local average noise and clutter power.

Based on the Neyman-Pearson lemma, The false alarm probability P_{fa} of the optimal detector can be described as follow the target model is Swerling I:

$$P_{fa}=P\left[Y>Y_0\,|\,H_0\right]=\int_{Y_0}^{\infty}\frac{1}{\mu}e^{-y/\mu}\,dy=\exp(-Y_0/\mu) \qquad \text{Eq. (6)}$$

And the detection probability is:

$$P_d=P\left[Y>Y_0\,|\,H_1\right]=\int_{Y_0}^{\infty}\frac{1}{\mu}e^{-y/\mu(1+s)}\,dy=P_{fa}^{\,1/(1+s)} \qquad \text{Eq. (7)}$$

Waveform Design and RDM Matrix

The basis of target detection is built on radar signal processing. In this section, a LFMCW radar system is considered to detect vehicles or pedestrians ahead and measure the relative velocity and range simultaneously. In this paper, the transmitted signal is defined as following form:

$$T(t)=\cos\left(2\pi\left(f_0t-\frac{Bt^2}{2T}\right)\right) \qquad \text{Eq. (8)}$$

Where f_0 is the LFMCW radar carrier frequency, B is the band width, T is the modulation period.

The rapid chirp waveform and signal processing scheme for the received chirp sequence is illustrated in figure 2.

The echo signal and the transmit signal are mixed to obtain the intermediate frequency signal. Then, the intermediate frequency signal is sampled and the RDM matrix is obtained after two FFT transformations.

The detailed process is as follows. In the first step, the first FFT is applied to each chirp signal and splits the radar Intermediate Frequency (IF) signal into different range gates. This procedure is repeated for each chirp signal and in total L FFT are processed. The result value will be stored column-wise in a two-dimensional matrix. In the second step, a second FFT is applied to each row of the two-dimensional matrix.

FIGURE 2 Echo signal processing and Radar target detection on RDM.

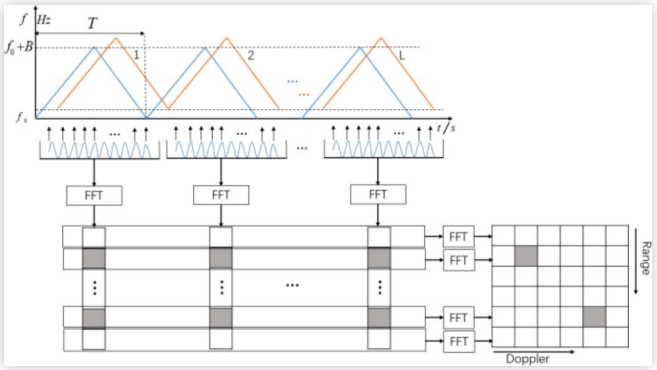

The complex valued output signal is stored in the so-called Range-Doppler-matrix (RDM). The target information is stored in this matrix, and the CFAR algorithm is processed to detect the target based on this RDM.

2-DAR Detector BASED on RDM

Combining several CAFR methods to improve overall performance is a trend in CFAR research. Rohling extends one-dimensional CA and OS CFAR to two-dimensional OS-CA CFAR, which greatly improves the robustness of target detection [10]. By adjusting the number of reference window and using CA method to estimate the posterior reference window, several generalized order statistics (GOS) CFAR detector are proposed by He You.et al, such as MOSCA [11], OSCAGO [12] and OSCASO [13] CFAR detector. One-dimension GOS CFAR implementation is shown in figure 3. The OS CFAR is applied in the front reference windows, while the CA CFAR is applied in the rear reference windows to estimate the local background noise and clutter power.

Based on the good characteristics of one-dimensional GOS CFAR in a multi-target environment, two-dimensional GOS-CA CFAR is established. The general idea is showed in figure 4. Most of radar targets can be considered as point

FIGURE 3 GOS CFAR adaptive detection scheme.

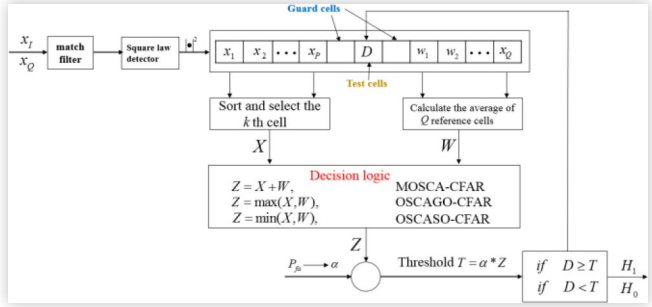

FIGURE 4 2-D sliding reference window design for GOS-CA CFAR.

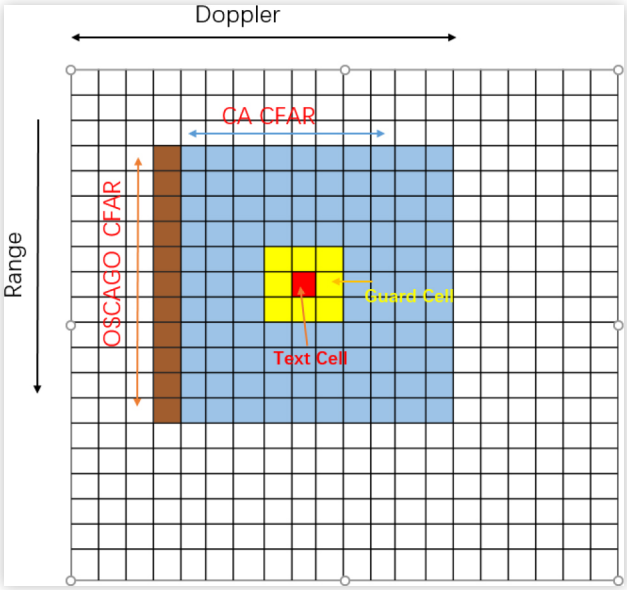

targets in range direction inside the RDM. However, targets like vehicles and pedestrians with relative velocity can be extended to Doppler direction. Therefore, at first, taking the detection cell as the center, local reference windows matrix is established to estimate the power of background noise and clutter. Then, The GOS CFAR is used in the range direction to avoid the masking effect in the multi-target environment and The CA CFAR procedure is applied in the Doppler direction to improve the noise level estimation accuracy. This combined scheme is called GOS-CA CFAR. In this case the GOS CFAR avoids all masking effects in multi-target situations and due to range direction specific sorting procedure and decision logic inside the two-dimensional reference window, the performance of GOS CFAR is significantly better than that of OS CFAR. Besides, the computation of GOS CFAR is about half of OS CFAR, which is easier to implement in practical engineering applications.

For a sampling. the RDM is a $M \times N$ matrix , and the element in column i, column j, is represented by Y_{ij}, as shown in figure4. Firstly, the estimated values of noise and clutter power Z_i in each column of the reference window are calculated. Secondly, these values are averaged to estimate the background noise power Z_{ij} as shown in following equation:

$$Z_{ij} = \begin{cases} \frac{1}{n}\sum_{j=1}^{n}\left(Y_j(k) + \frac{1}{Q}\sum_{q=1}^{Q} Y_q \right) & MOSCA-CA \\ \frac{1}{n}\sum_{j=1}^{n}\left(\max\left(Y_j(k), \frac{1}{Q}\sum_{q=1}^{Q} Y_q \right) \right) & OSCAGO-CA \\ \frac{1}{n}\sum_{j=1}^{n}\left(\min\left(Y_j(k), \frac{1}{Q}\sum_{q=1}^{Q} Y_q \right) \right) & OSCASO-CA \end{cases} \quad \text{Eq. (9)}$$

Threshold for each cell is:

$$T_{ij} = \alpha Z_{ij} \quad \text{Eq. (10)}$$

Then, the threshold matrix can be obtained. Finally, each element of the two matrix will be compared according to the target discrimination criterion mentioned above, so the target can be extracted if it really exists in RDM.

In order to evaluate the performance of the CFAR detectors, a nominal quantity average decision threshold (ADT) was defined by Rohling [7]. ADT is an optional metric for computing loss of detection performance. For a given P_{fa} and N, ADT is independent of detection probability. And the smaller the value of ADT, the better the detection performance, that is, the higher detection performance. Therefore, to evaluate and compare the detection performance of the different CFAR procedures analyzed in this paper, the ADT is considered.

The scaling factor α and the average decision threshold ADT can be calculated based on Monte Carlo simulations for the GOS-CA CFAR, when the parameters P_{fa}, P, Q and k are determined. The reference window length P is suggested to select 12-16 or greater, and the rank-order k in suggested to Select between 1/2P and 3/4P According to Ref.[7]. The formulas for P_{fa}, ADT of GOS-CA and OS-CA CFAR are shown in Appendix.

The parameters are set to P = 16, Q = 16, $P_{fa} = 10^{-6}$. After Monte Carlo simulation, the results are shown in following tables

As it can be seen from table 2 ,when the CFAR parameters are the same, the value of ADT_{OS} is higher than that of other three detectors. That is, the performance of the OS CFAR detector is worse than that of the GOS CFAR detector. Here are the methods for selecting parameters k and α in simulation experiments: when the P, Q and P_{fa} are determined, the k and α should be chosen corresponding to the ADT values at the minimum. So, in this section, the 2-D GOS-CA CFAR model is built and the process of parameter selection is introduced.

TABLE 1 Scaling factor α for CFAR for $P_{fa} = 10^{-6}$.

k	MOSCA	OSCAGO	OSCASO	OS
6	13.3	20.8	120.3	120.4
7	12.4	19.8	79.5	79.4
8	11.6	18.9	56.3	56.6
9	10.3	18.2	42.1	42.4
10	9.6	16.8	33.2	32.9
11	8.8	15.6	26.7	26.1
12	7.9	14.6	23.4	20.9
13	7.4	13.0	22.1	13.7
14	6.8	11.8	21.6	10.9

TABLE 2 Average Decision Threshold (ADT) for CFAR for $P_{fa} = 10^{-6}$.

k	MOSCA	OSCAGO	OSCASO	OS
6	19.3	20.7	53.9	54.4
7	19.1	20.4	42.7	43.8
8	18.9	19.6	35.6	37.5
9	18.6	19.2	30.6	33.4
10	18.5	19.0	26.4	30.6
11	18.3	19.3	23.3	28.6
12	18.4	19.7	21.7	27.2
13	18.6	20.7	21.3	26.2
14	18.8	21.9	21.7	25.7

Simulation Experiment Analysis

In this section, a numerical simulation is conducted to demonstrate and evaluate the performance of the proposed algorithm in multi-target environment. the 2-D GOS-CA CFAR detectors (MOSCA-CA, OSCAGO-CA, OSCAGO-CA) are compared to the 2-D OS-CA CFAR in multi-target environment. The performances are evaluated in sense of detection probability taking under control the desired false alarm probability.

The following work is based on the working condition of automotive millimeter wave radar on the road. It is assumed that three are eight targets in front of the automotive radar with different velocity and distance and their fluctuation characteristic is Swerling I. The echo signal of these eight targets is superposition with ground clutter and heat noise, so the background noise and clutter is closed to the Rayleigh distribution after square law filter. In the following simulations, The signal-to-noise ratio (SNR) of target and noise is set to 10dB, and the parameters selection in case of the false alarm probability $P_{fa} = 10^{-6}$ are shown in the table.3.

After 20 times of simulation experiment. one of the simulation results is shown as follow.

As shown in the figure 5.6.7.9. The middle surface layer is threshold matrix, and only when the value in the RDM matrix is greater than the threshold at the same location will the object be recognized as the target. However, when the FFT sampling points are too large, a target will occupy several cells of the RDM, which brings difficulties to the target detection, and also raises the false alarm probability.

TABLE 3 Parameters for CFAR for $P_{fa} = 10^{-6}$.

	MOSCA	OSCASGO	OSCASO	OS
P	16	16	16	16
Q	16	16	16	16
k	11	10	13	26
α	8.8	16.8	22.1	13.7

FIGURE 5 Simulation result of 2-D MOSCA-CA CFAR target detection.

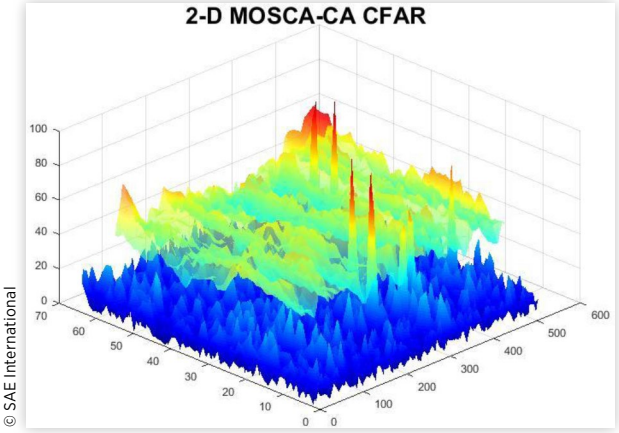

FIGURE 6 Simulation result of 2-D OSCAGO-CA CFAR target detection.

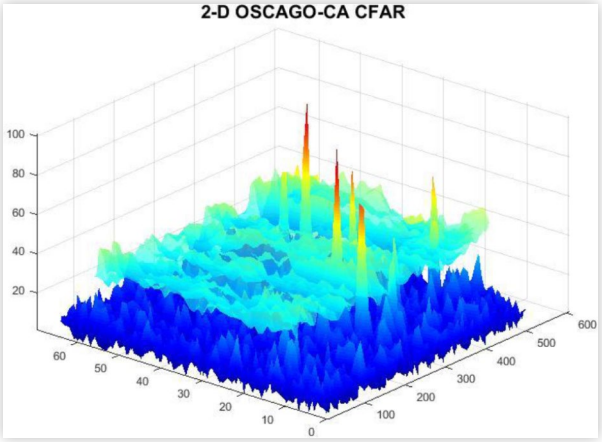

FIGURE 7 Simulation result of 2-D OSCASO-CA CFAR target detection.

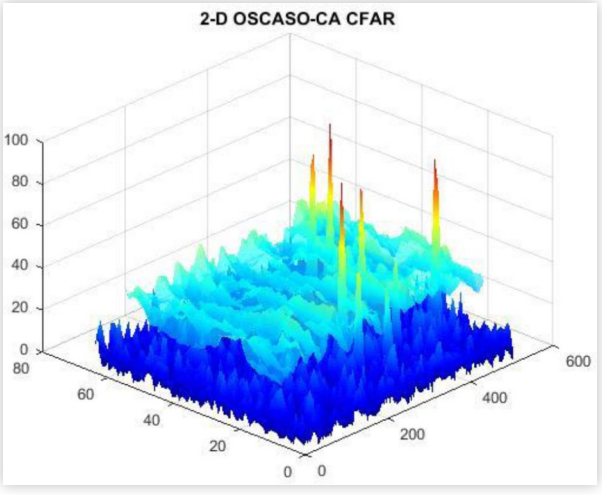

FIGURE 8 Target detection result of 2-D GOS-CA CFAR.

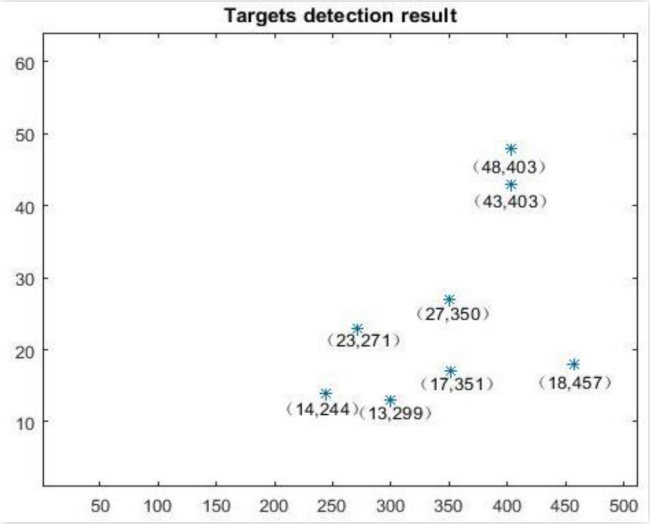

FIGURE 9 Simulation result of 2-D OS-CA CFAR target detection.

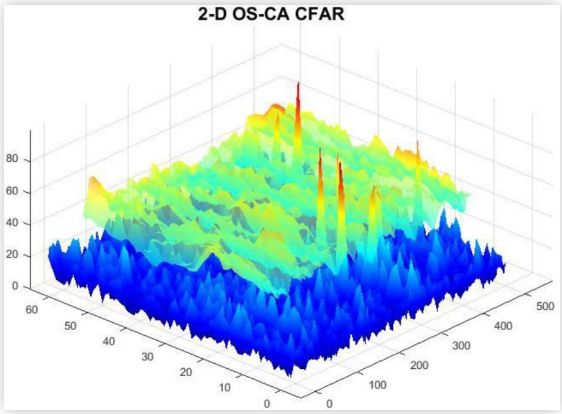

FIGURE 10 Target detection result of 2-D OS-CA CFAR.

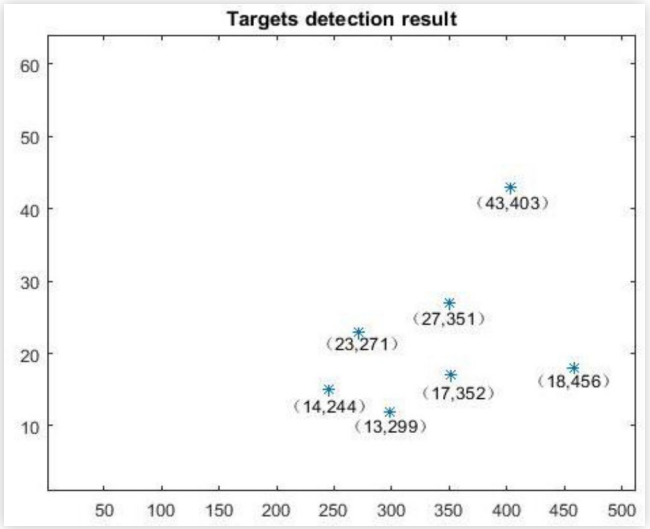

The position of the target can be obtained through the information clustering processing. The process is based on two hypotheses: Each cell contains only one target's information; Each target occupies only one cell of RDM, that is, the target cell has more signal power than any cell adjacent to it. By clustering processing, the target coordinates are obtained accurately in RDM.

Through these simulation results, we find that the 2-D GOS-CA CFAR proposed in this paper can accurately detect the targets without any missing or false detection. However, one target is missed by the 2-D OS-CA detector when the location of multiple targets is very close. That is because when the reference windows contain multiple targets, the threshold of the background noise estimation is raised. This cannot be completely solved by a single sorting process. In this case, the robustness for target detection is improved by varying the number of front and rear reference windows, or adding a variety of logical decisions.

When the other parameters are determined, the detection probability P_d of the targets will change with SNR. When the background noise and clutter satisfy Rayleigh distribution, the equations of the detection probability P_d of the GOS-CA CFAR and OS-CA CFAR are shown in Appendix.

The P_d comparison of the 2-D GOS-CA CFAR and 2-D OS-CA CFAR in multi-interfering targets environment is shown in Figure.11.

As it can be seen from the figure.11 that P_d of the GOS-CA CFAR is upper to OS-CA CFAR in multi-target environment. P_d of the OSCAGO-CA and OSCASO-CA CFAR is upper to 98% and better as about 3% than MOSCA-CA CFAR when SNR=25dB. The result show that the GOS-CA CFAR has better detection performance in multi targets environment under the given simulation parameters in this paper.

FIGURE 11 P_d comparison between detectors in multi-target environment.

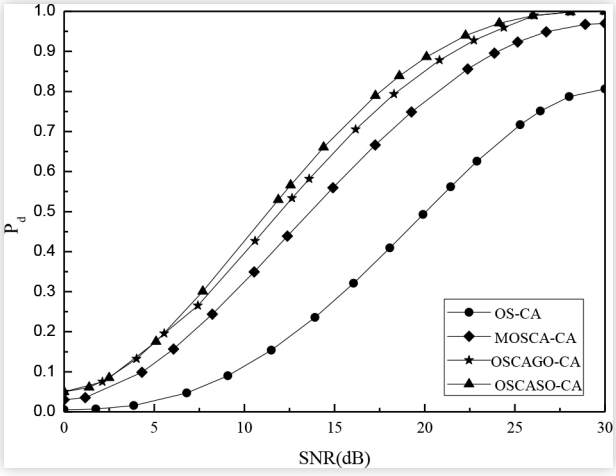

Summary and Future Work

In this paper, a new 2-D GOS-CA CFAR detector based on generalized statistics is proposed to improve the detection performance of vehicle automotive millimeter wave radar in multi-target environment. The design concept of this 2-D CFAR detector comes from 2-D OS-CA CFAR proposed by Rohling. Besides, the robustness of 2-D GOS-CA CFAR is much better than that of 2-D OS-CA CAFR, especially when the number of targets is large. Moreover, in terms of computational complexity, when the number of reference sliding windows is the same, the sorting cells of the GOS-CA CFAR detector are about half of that of the OS-CA CFAR detector. The computation time is greatly reduced so it is easier to implement in hardware design. Each CFAR detector has its own advantages in a particular detection environment. So, by combining the advantages of several detectors, adding decision logic, and changing the sliding window parameters, the detection robustness of the CFAR detector can be improved in a variety of conditions. This is also design idea of the new CFAR detector.

In the following work, more simulation experiments will be carried out in order to get the Optimal parameters of 2-D GOS-CA CFAR detector. And clutter edge environment will be taken into account

Contact Information

Li Sen
Work phone: (86)18516705739 /(86)18101912989
lisen@tongji.edu.cn

Acknowledgments

National Key R&D Program of China 2016YFB0100901

References

1. Finn, H. M., and Johnson R. S. "Adaptive detection mode with threshold control as a function of spatially sampled clutter- level estimates." *RCA review* 29 (1968): 414-464.
2. Hansen, V. Gregers. "Constant false alarm rate processing in search radars(receiver output noise control)." *Radar- Present and future* (1973): 325-332.
3. Trunk, Gerard V. "Range resolution of targets using automatic detectors." *IEEE Transactions on Aerospace and Electronic Systems* 5 (1978): 750-755.
4. Barkat, M., and Varshney P. K. "A weighted cell-averaging CFAR detector for multiple target situations." *Proceedings of the Twenty-First Annual Conference on Information Sciences and Systems*. 1987.
5. Barkat, M., Himonas S. D., and Varshney P. K. "CFAR detection for multiple target situations." *IEEE Proceedings F-Radar and Signal Processing*. Vol. 136. No. 5. IET, 1989.
6. Zhang, Renli, et al. "An improved CFAR detector for non-homogeneous clutter environment." *Signals Systems and Electronics (ISSSE), 2010 International Symposium on*. Vol. 2. IEEE, 2010.
7. Rohling, Hermann. "Radar CFAR thresholding in clutter and multiple target situations." *IEEE transactions on aerospace and electronic systems* 4 (1983): 608-621.
8. Rohling, Hermann. "Ordered statistic CFAR technique-an overview." *Radar Symposium (IRS), 2011 Proceedings International*. IEEE, 2011.
9. Rickard, John T., and Dillard George M. "Adaptive detection algorithms for multiple-target situations." *IEEE Transactions on Aerospace and Electronic Systems* 4 (1977): 338-343.
10. Kronauge, Matthias, and Rohling Hermann. "Fast two-dimensional CFAR procedure." *IEEE Transactions on Aerospace and Electronic Systems* 49.3 (2013): 1817-1823.
11. You H, Jian G, Yingning P, et al. "A new CFAR detector based on ordered statistics and cell averaging". *CIE 1996 International Radar Conference of*. IEEE, 1996: 106-108.
12. You H, Jian G, "A new CFAR Detector with Greatest of Selections". *IEEE 1995 International Conference on Radar*, Alexandria, Virginia, USA, 1995:589-591.
13. You H, Jian G, Rohling H. "Two new CFAR detectors based on maximum and minimum selection". *Journal of Systems Engineering and Electronics*. 1995,17(7):6-16.

Appendix

The related derivations can be found in Ref. [7], [11], [12], [13]

1. ADT function

$$ADT_{(OS-CA)} = \frac{E(\alpha Z)}{\mu} = \alpha \sum_{i=1}^{k} \frac{1}{P-k+i} \quad \text{Eq. (11)}$$

$$ADT_{(MOSCA)} = \alpha \left[\sum_{i=1}^{k} \frac{1}{P-k+i} + 1 \right] \quad \text{Eq. (12)}$$

$$ADT_{OSCAGO} = \alpha \left[\sum_{i=1}^{k} \frac{1}{P-k+i} - \frac{1}{Q^2} k \binom{P}{k} \sum_{i=0}^{Q-1} (i+1) \sum_{j=0}^{k-1} \binom{k-1}{j} (-1)^j \times \left(\frac{Q}{P+1-k+j} \right)^{i+2} + \sum_{i=k}^{P} \binom{P}{i} \right] \sum_{j=0}^{i} \binom{i}{j} (-1)^j \left(\frac{Q}{P+j-i} \right)^{O+1} \quad \text{Eq. (13)}$$

$$ADT_{(OSCAGO)} = \alpha \left[1 + \frac{1}{Q^2} k \binom{P}{k} \sum_{i=0}^{Q-1} (i+1) \sum_{j=0}^{k-1} \binom{k-1}{j} (-1)^j \left(\frac{Q}{P+1-k+j} \right)^{i+2} - \sum_{i=k}^{P} \binom{P}{i} \sum_{j=0}^{i} \binom{i}{j} (-1)^j \left(\frac{Q}{Q+j-i} \right)^{Q+1} \right] \quad \text{Eq. (14)}$$

2. Detection probability function

$$P_{d(OS)} = k \binom{P}{k} \frac{\Gamma[P-k+1+\alpha/(1+SNR)]\Gamma(k)}{\Gamma[P+\alpha/(1+SNR)+1]} \quad \text{Eq. (15)}$$

$$P_{d(MOSCA)} = k \binom{P}{k} \frac{\Gamma[P-k+1+\alpha/(1+SNR)]\Gamma(k)}{\Gamma[P+\alpha/(1+SNR)+1]} \frac{1}{\left[1 + \frac{\alpha}{(1+SNR)Q} \right]^P} \quad \text{Eq. (16)}$$

$$\begin{aligned} P_{d(OSCAGO)} = {} & \frac{P!\Gamma[P-k+\alpha/(1+SNR)+1]}{(P-k)!\Gamma[P+\alpha/(1+SNR)+1]} - k \binom{P}{k} \frac{1}{Q} \sum_{i=0}^{Q-1} \sum_{j=0}^{k-1} \binom{k-1}{j} (-1)^j \\ & - \left[\frac{Q}{P+1-k+j+\alpha/(1+SNR)} \right]^{i+1} + \sum_{i=k}^{P} \binom{P}{i} \sum_{j=0}^{i} \binom{i}{j} (-1)^j \times \left[\frac{Q}{P+j-i+\alpha/(1+SNR)} \right]^Q \end{aligned} \quad \text{Eq. (17)}$$

$$\begin{aligned} P_{d(OSCASO)} = {} & \frac{1}{[1+\alpha/Q(1+SNR)]^Q} + k \binom{P}{k} \frac{1}{Q} \sum_{i=0}^{Q-1} \sum_{j=0}^{k-1} \binom{k-1}{j} (-1)^j \\ & \times \left[\frac{Q}{P+1-k+j+\alpha/(1+SNR)} \right]^{i+1} - \sum_{i=k}^{P} \binom{P}{i} \sum_{j=0}^{i} \binom{i}{j} (-1)^j \left[\frac{Q}{P+j-i+\alpha/(1+SNR)} \right]^Q \end{aligned} \quad \text{Eq. (18)}$$

3. False alarm rate function

$$P_{fa(OS-CA)} = k\binom{P}{k}\frac{\Gamma(P-k+1+\alpha)\Gamma(k)}{\Gamma(R+\alpha+1)} \quad \text{Eq. (19)}$$

$$p_{fa(MOSCA)} = k\binom{P}{k}\frac{\Gamma(P-k+1+\alpha)\Gamma(k)}{\Gamma(P+\alpha+1)(1+\alpha/Q)^{Q}} \quad \text{Eq. (20)}$$

$$P_{fa(OSCAGO)} = \frac{P!\Gamma(P-k+\alpha+1)}{(P-k)!\Gamma(P+\alpha+1)} - k\binom{P}{k}\frac{1}{Q}\sum_{i}^{Q-1}\sum_{j=0}^{k-1}\binom{k-1}{j}(-1)^{j}\times\left[\frac{Q}{P+1-k+j+\alpha}\right]^{i+1} + \sum_{i=k}^{P}\binom{P}{i}\sum_{j=0}^{i}\binom{i}{j}(-1)^{j}\left[\frac{Q}{P+j-i+\alpha}\right]^{Q} \quad \text{Eq. (21)}$$

$$P_{fa(OSCASO)} = \frac{1}{(1+\alpha/Q)^{Q}} + k\binom{P}{k}\frac{1}{Q}\sum_{i=0}^{Q-1}\sum_{j=0}^{k-1}\binom{k-1}{j}(-1)^{j}\left(\frac{Q}{P+1-k+j+\alpha}\right)^{i+1} - \sum_{i=k}^{P}\binom{P}{i}\sum_{j=0}^{i}\binom{i}{j}(-1)^{j}\left(\frac{Q}{P+j-i+\alpha}\right)^{Q} \quad \text{Eq. (22)}$$